JOURNAL OF MATERIALS SCIENCE 31 (1996) 905–914

Subsurface damage in alumina induced by single-point scratching

I. ZARUDI, L. ZHANG*, Y.-W. MAI
Center for Advanced Materials Technology, Department of Mechanical and Mechatronic Engineering, The University of Sydney, New South Wales 2006, Australia

Damage-free processes of grinding of brittle materials have been widely used in industry for producing electronic and optical components with high surface integrity. It has been found that the transition threshold from ductile flow to brittle fracture during the process of material removal plays a central role in the quality control of a machined surface. However, the precise microscopic mechanism which governs the formation of dislocation structure and micro-cracking when machining a brittle material such as alumina, remains unclear. The mechanism of formation and structure of the plastic or damage zones in alumina of two different grain sizes (1 and 25 μm) subjected to single-point scratching with sharp and blunt indenters were studied in this paper. Using transmission electron microscopy, characteristic features of the plastic/damage zone in terms of loading conditions and microstructure of the materials were carefully investigated. It was found that the grain size and the geometry of the indenter had a great effect on the dislocation structure of the plastic zone and that the subsurface damage could be very severe, even though the machined surfaces appeared damage-free. These results indicate that the ductile flow to brittle fracture transition in machining brittle ceramics is more complicated than previously thought and that a reliable criterion has yet to be established to predict a real damage-free grinding process.

1. Introduction

To produce satisfactory ceramic components of high precision and high surface integrity, machining processes such as grinding must be conducted in a damage-free regime so that material removal is without micro-cracking both on the surface and in the subsurface [1]. Extensive studies [2–5] have been carried out to demonstrate the effect of machining parameters, such as the depth of cut, loop stiffness of machines, properties of coolant, and so forth. In all these investigations, the damage-free regime was said to be achieved if a smooth and damage-free machined surface was obtained when examined by a scanning electron microscope. Indeed, this procedure has been commonly adopted and used as a criterion of damage-free machining by both researchers and manufacturing engineers. From the point of view of deformation of materials, however, the mechanisms of transition from ductile flow to brittle fracture are far from being fully understood. Specifically, to the authors' knowledge, the slip systems of dislocations induced by the cutting edges and their relations with microcracking are unclear.

The process of material removal in a grinding operation could be viewed, to a great extent, as an integration of a set of single-point cuts [5–8]. Therefore, an investigation into the material's response to single-point scratching would offer an insight into the deformation mechanisms caused by grinding. Relevant past studies on single-point scratching covered mainly the following aspects: topography of scratched surfaces [9, 10], microfracture and deformation phenomena [11, 12], and determination of coefficient of friction and hence the ratio of normal to tangential forces [12]. Again, as mentioned above, the mechanism of material removal was classified as brittle fracture or plastic deformation [13, 14] just according to the surface topography of the scratched groove. Also, although previous studies on indentation of brittle materials, both theoretical and experimental [15–17], have examined in detail the deformation mechanisms under the indenter and, to a certain degree, material removal processes, these are not entirely relevant to the machining operation, which is the subject of interest in this paper.

The brittle nature of ceramics is generally considered to be the main reason for the lack of plastic deformation. There is little or no plasticity involved in the bond-rupture process. Most cracks are dislocation-free [18] and only a few cracks are considered to be caused by interfacial mismatch dislocations [19]. Take alumina as an example. The possibility of plastic deformation of alumina at room temperature induced by indentation and abrasion has long been doubted

*Author to whom all correspondence should be addressed.

0022–2461

[20], as this material has ionic/covalent bonding which limits the number of independent slip systems. Also, the critical temperature causing the brittle to ductile transition in alumina is higher than $0.5T_M$ ($T_M \approx 2000\,°C$ is the melting temperature). Therefore, it seems unlikely that a sufficient number of slip systems would be activated at room temperature to make possible homogeneous plastic deformation. However, Peter *et al.* [21] recently found that if a hydrostatic pressure was applied, plastic deformation in sapphire could be achieved at a temperature much lower than the above critical transition temperature. In this case, the systems of prism plane slip at 200 °C and basal slip at 400 °C were detected. This might be related to the observations of Hockey and Lawn [18] who, with the aid of transmission electron microscopy, found a high density of dislocations and twins in sapphire at room temperature, as the indenter would create a high hydrostatic stress in the indented zone.

Clearly, existing results are insufficient to explain the fundamental mechanisms of deformation of a whole class of ceramics in the regime involving ductile–brittle transition in relation to the processes of material removal. Therefore, the present work aimed to investigate the microstructure of the subsurface of alumina subjected to single-point scratching and to provide essential information for further study of damage-free grinding. As the first step, we examined in detail the different mechanisms caused by two different grain sizes of an alumina under different scratching conditions.

2. Experimental procedure

Polycrystalline alumina specimens were made from commercially available alumina powder of 99.99% purity (Morimura Brothers Inc., Tokyo). Sintering was carried out in air at 1300–1700 °C for 2–18 h depending on the grain size required. Specimens with two grain sizes, 1 and 25 μm, respectively, were used to demonstrate the grain-size effect when all other test conditions were the same. The scratching experiments were conducted on a reciprocating sliding machine, the details of which were given elsewhere [9]. Two types of indenter, a blunt diamond conical indenter of about 100 μm tip radius and a sharp Vickers pyramid indenter with an included angle 136°, were used to give different contact conditions of scratching. Specimens measuring $10 \times 6 \times 4\,mm^3$ were used after polishing that was carried out in two steps using diamond pastes of two different particle size with average diameters of 3 and 1 μm respectively. The normal load applied was 6 N and the sliding speed of the indenter was $6\,mm\,s^{-1}$. Tangential forces during scratching were measured with a linear variable displacement transducer (LVDT).

The microstructure of the subsurfaces of specimens was examined by a transmission electron microscope (TEM) Philips EM430 operating at 300 kV. To do this, a scratched specimen was first sectioned into thin slices, 1 mm thick, perpendicular to the scratched groove, Fig. 1a. Two slices were glued together in the manner shown in Fig. 1b and thinned down first mechanically and then by ion milling to a thickness of 40 nm suitable for TEM study. If the plastic or damaged zone was not fully revealed the specimen was thinned down again using the same procedure until the full area of damage could be clearly seen. This method of specimen preparation enabled us to investigate the subsurface damage thoroughly in a plane perpendicular to the scratched surface, and therefore detect subsurface structure immediately below the surface and to identify changes in the structure due to deformation. Such cross-sections were also examined using a scanning electron microscope (SEM) JM505 to reveal the dimensions of any possibly damaged regions.

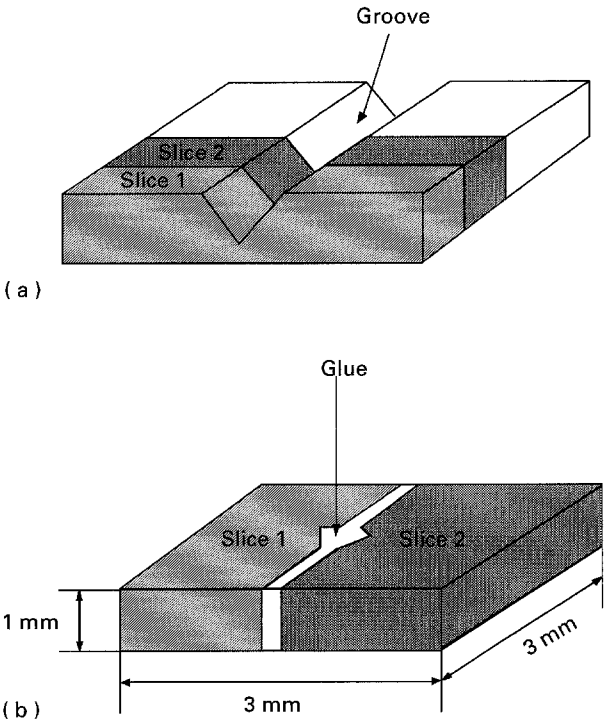

Figure 1 Preparation of specimens for TEM investigations: (a) cutting into thin slices; (b) gluing two slices together.

3. Results and discussion

3.1. The initial microstructure of alumina

Examination of the microstructure revealed that the density of dislocations was extremely low in the coarse-grained (25 μm) alumina. The majority of grains were dislocation-free, Fig. 2a. The porosity of the material was also very clear. A tooth-like structure was, however, observed at the grain boundaries, Fig. 3a, which could be identified as stacking faults. The high density of such faults at the grain boundaries shows the existence of residual stresses in the coarse-grained alumina after sintering.

In contrast, the fine-grained alumina (1 μm) was very inhomogeneous in grain size (Fig. 2b). It varied from 0.8–5 μm with an average value of 1 μm. Porosity was also obvious among the grains. Similar to the coarse-grained alumina, no dislocations were detected inside the grains. However, no tooth-like structure was observed at the grain boundaries (Fig. 3b). This indicates that the residual stresses in the fine-grained alumina due to sintering are much smaller.

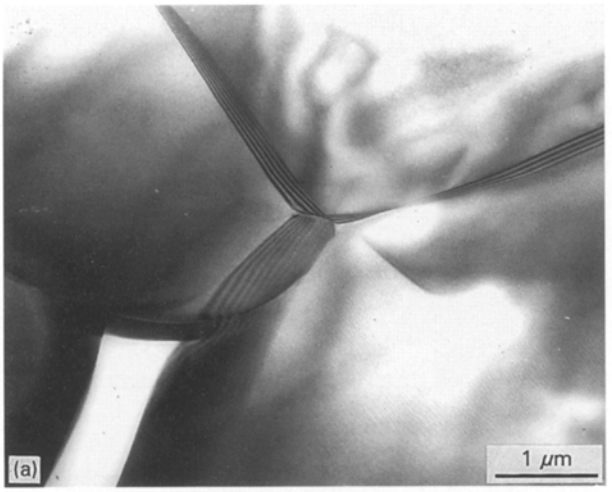

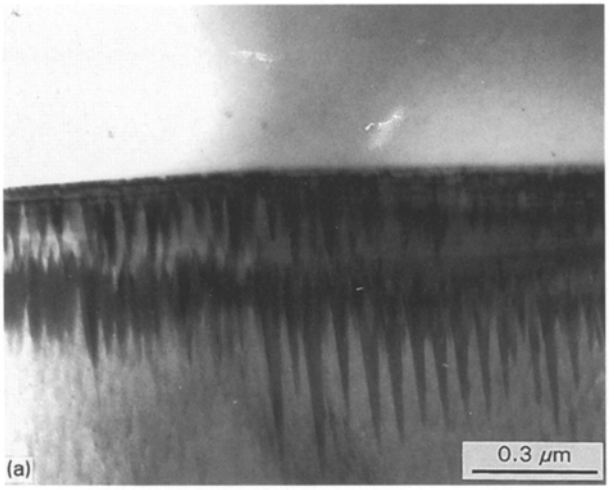

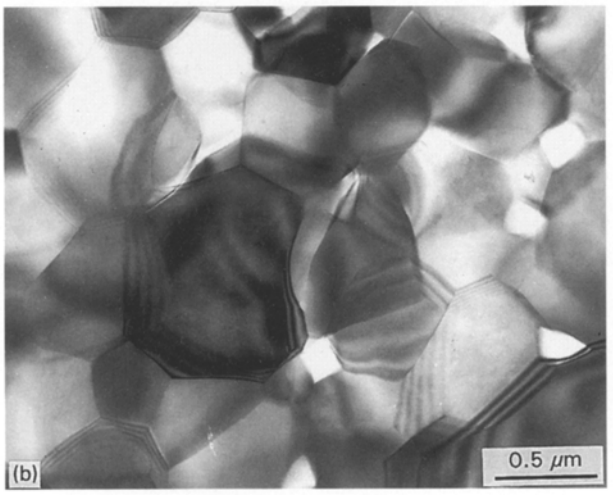

Figure 2 The initial microstructure of alumina after sintering: (a) 25 μm grains; (b) 1 μm grains. Grains are dislocation-free.

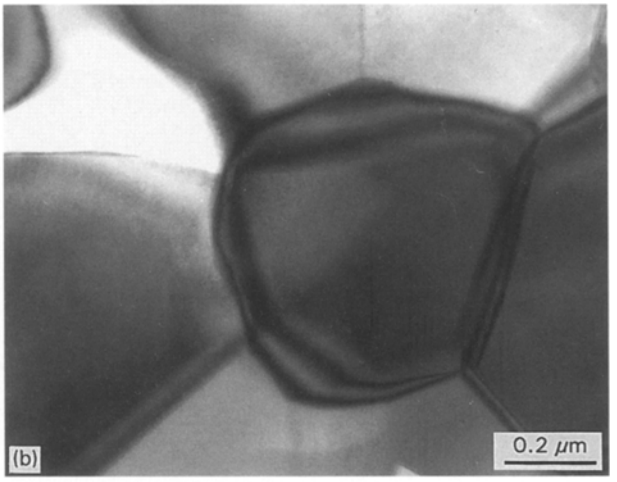

Figure 3 The structure of grain boundaries of alumina after sintering: (a) 25 μm grains; (b) 1 μm grains. Tooth-like structure is clearly seen at grain boundaries of the coarse-grained ceramic.

3.2. Subsurface microstructure due to polishing

The surface of a polished coarse-grained alumina specimen prepared for the scratching experiments was smooth with only a few grains fractured due to polishing. There was a layer of high dislocation density about 0.5 μm thick beneath the polished surface (Fig. 4a). On the other hand, for the fine-grained alumina the polished surface (Fig. 4b) was very smooth. No grains were broken during polishing and no dislocations were detected on the subsurface of the polished specimen even though the polishing procedure was the same as for the coarse-grained alumina. This indicates that dislocation initiation is much harder in the fine-grained alumina.

3.3. Structure of the subsurface after scratching

3.3.1. Scratching with a sharp indenter

3.3.1.1. Coarse-grained alumina. The topography of the groove, Fig. 5a, shows that grains were fractured and even dislodged during scratching. The profile of the groove was irregular and differed from that of the indenter whose width and depth were both about 20 μm, see Figs 5a and 6a. (The width of the groove is more than 20 μm in Fig. 6a due to fractured and dislodged grains). The damage region was clearly seen in the scanning electron micrograph of a cross-section perpendicular to the groove (Fig. 5b). It was hemispherical with an approximate radius of 80 μm and was characterized by a high density of cracks running between the grains which were almost separated.

The structure of the material at the bottom of the groove is shown in Fig. 6. A severely deformed zone could be observed. The deformed structure was complex, containing a high density of dislocations, deformation twins and a large number of cracks (Fig. 6b–d). This zone spread to a distance of about two grains (20–40 μm) from the border of the groove and contained many dislocation bands (Fig. 6c). It was impossible to resolve the individual dislocations in the bands. Rhombohedral twins were also detected (Fig. 6d) with a high density of dislocations near their boundaries.

A preliminary contrast analysis using various diffracting conditions verified that different slip systems were activated during scratching. Triple junctions

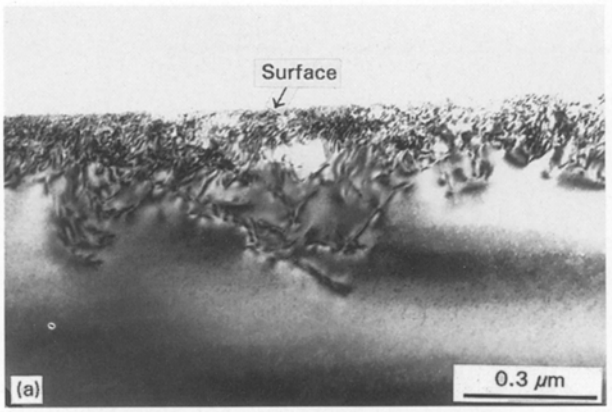

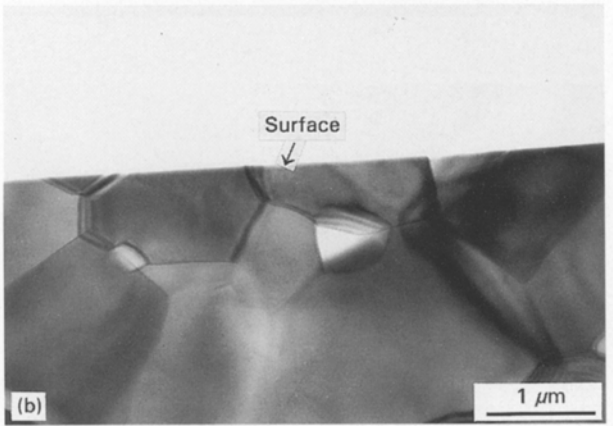

Figure 4 Subsurface structure of alumina after polishing: (a) 25 μm grains; (b) 1 μm grains. Note the subsurface layer with a high density of dislocations in the coarse-grained alumina.

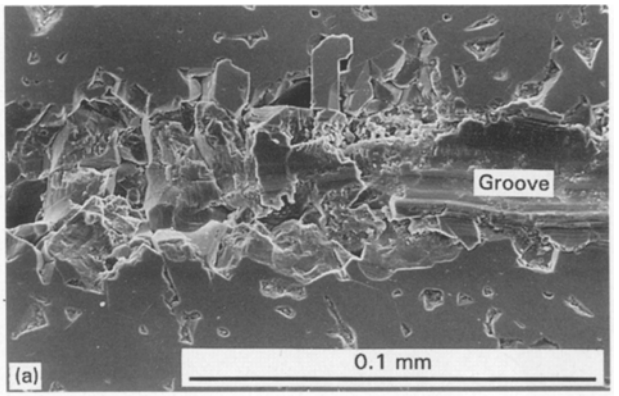

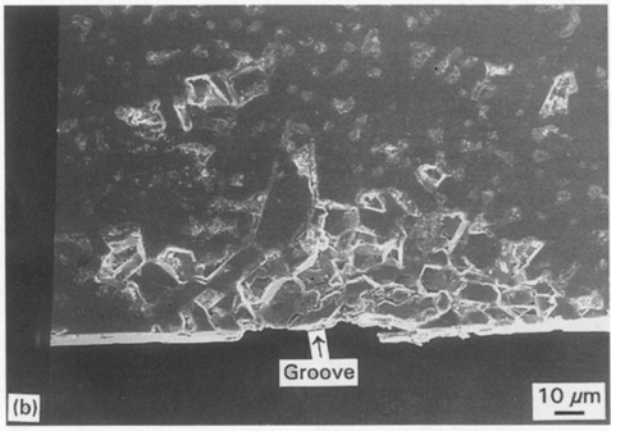

Figure 5 Coarse-grained alumina after scratching with a sharp indentor. (a) Topography of the groove, and (b) subsurface damage.

detected in the region examined also confirmed this conclusion. Cracks developed between and through the grains. The initial structure was so heavily damaged that it was impossible to determine individual features of the structure where cracks were formed.

3.3.1.2. Fine-grained alumina. The topography of the scratched surface of the fine-grained alumina is shown in Fig. 7a. The groove was smooth but radial cracks could be clearly seen on the surface near the groove. The included angle of the groove was about 150° (Fig. 8a) which was larger than that of the indenter (136°) because of the elastic recovery of the alumina.

Almost no separation of grains occurred during scratching of the fine-grained alumina. In fact, the density of defects was lower at the grain boundaries because the initiation of cracks between grains was harder and thus grain separation was more difficult. Only a limited number of cracks was found beneath the first row of grains. The median cracks, however, were formed at a distance of 5–6 μm below the surface, Fig. 8b. The length of the median cracks was about 15 μm, and was approximately the size of the damage zone. The damage region in the fine-grained alumina was four times smaller than that in the coarse-grained alumina.

The structure of the plastic or damage zone underneath the groove bottom from which median and radial cracks emanated could be examined in Fig. 8b–d in more detail. The grains in the surface layer of about 1 μm thick were severely deformed (Fig. 8c). The density of dislocations was comparable to that in the coarse-grained alumina. A few grains below, there was a highly deformed layer but with a much lower dislocation density (Fig. 8d), where individual dislocations and dislocation loops could be clearly distinguished. Fig. 8d shows the centre of a dislocation loop located at the boundary of a grain. Accordingly, the dislocation source was at the grain boundary, which could be created by grain sliding via extended loading. No cracks went through the grains. Twins appeared only occasionally. Immediately below this layer (about 5 μm below the surface), a median crack was formed (Fig. 8b) which propagated mainly along grain boundaries. Although the median crack was initiated in the deformed layer, it grew quickly through the region without detectable deformation. No separation of grains took place in the whole process.

As mentioned before, the plastic or damage zone in the coarse-grained alumina was characterized by both a high dislocation density and the appearance of rhombohedral twins. In addition, the dislocation distribution was very inhomogeneous. At the same time, many transgranular and grain-boundary cracks were formed. Therefore, the main difference in the structure

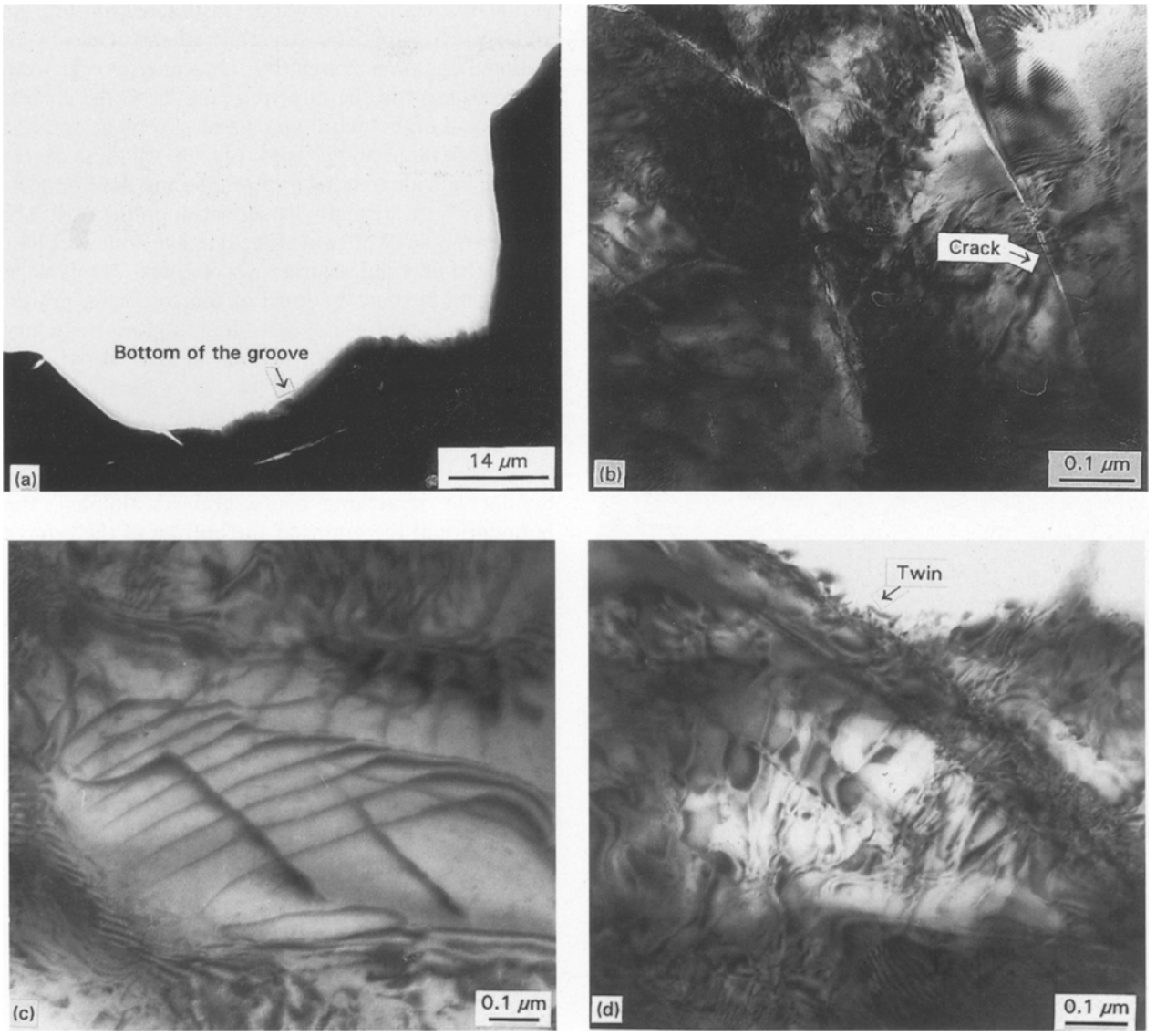

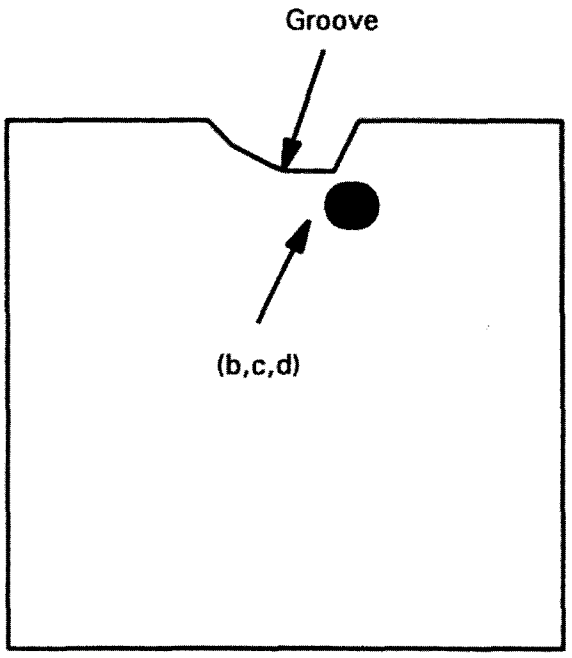

Figure 6 Scratching test with a sharp indenter on 25 μm coarse-grained alumina. (a) General view of groove profile. Note the irregular form of the groove. (b) The highly deformed zone under the groove with cracks. (c) Dislocation structure of the plastic zone. Note regions with high and low dislocation densities. (d) Rhombohedral twins in the plastic zone.

of the plastic or damage zones of the fine- and coarse-grained aluminas was the formation of rhombohedral twins and inhomogeneity of dislocation distribution. It is well known that inhomogeneous distribution of dislocations is not favourable for crack resistance and that the appearance of twins would cause additional cracking. Furthermore, the interaction of rhombohedral twins may nucleate macroscopic cracks [21]. The same effect could be observed for intersecting twins with grains boundaries. It then follows that in the fine-grained alumina, the homogeneous distribution of dislocations in the severely deformed layer and the low density of dislocations in the lightly deformed layer cooperatively increase the crack resistance of the material. Hence, the fine-grained alumina has a higher ductile–brittle transition threshold; though it should be noted in the case studied that median/radial cracks do occur (Figs 7a and 8b).

3.3.2. Scratching with a blunt indenter

3.3.2.1. Coarse-grained alumina. Unlike what happened in the experiments with the sharp indenter, the groove generated by the blunt indenter was very

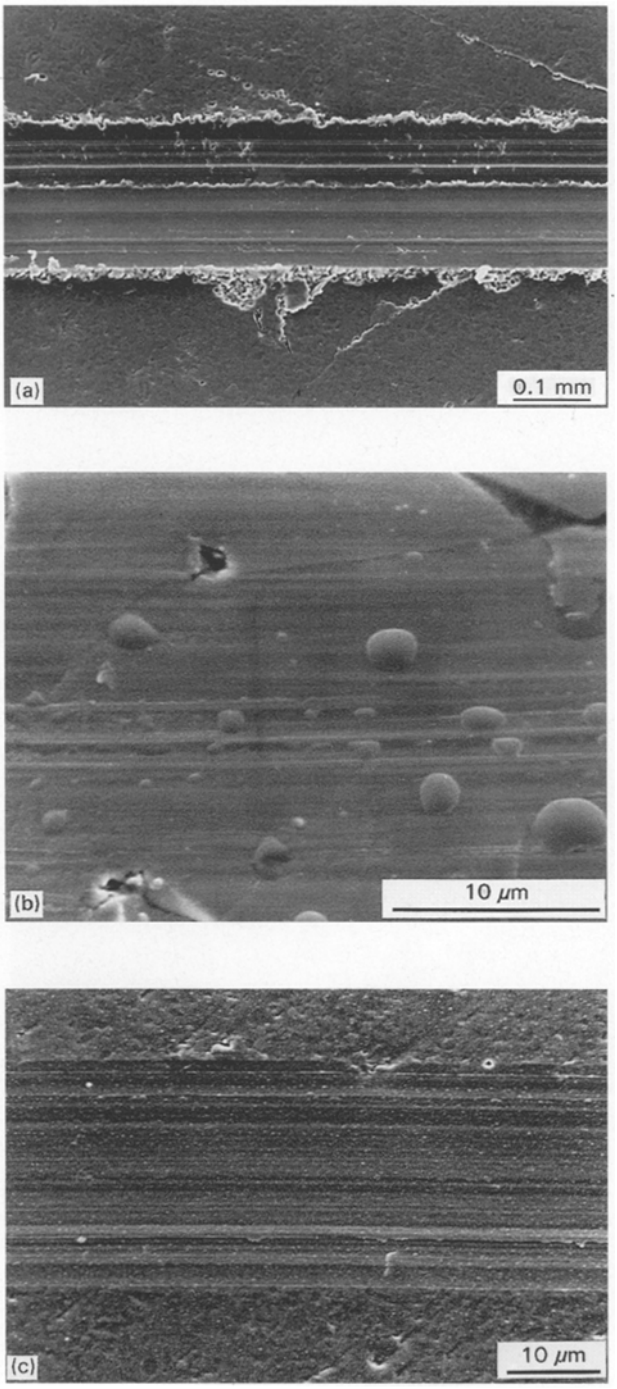

Figure 7 Topography of the surface after scratching. (a) Fine-grained alumina, sharp indenter; (b) coarse-grained alumina, blunt indenter; (c) fine-grained alumina, blunt indenter.

smooth, Figs 7b and 9a, with a depth of about 9 μm and a width of 20 μm. However, this does not mean that the deformation of material is purely plastic. TEM examinations of the cross-section perpendicular to the scratched groove showed that cracks were developed beneath the first row of grains. The blunt indenter also created many microcracks inside the grains (i.e. transgranular cracks) in the severely deformed layer. The structure of the damage zone had a distinct feature compared with that formed by the sharp indenter. Many rhombohedral twins appeared in the severely deformed layer, Fig. 9b. Moreover, the density of dislocations was low and therefore individual dislocations could be distinguished, Fig. 9c, and the characteristic structure where cracks were initiated could be recognized. Thus microcracks were found to form in the direction parallel to the corresponding rhombohedral twins and slip planes and at the sites of intersecting twins, Fig. 9b. All these observations indicate that the appearance and development of cracks were strongly dependent upon the existence and morphology of twins. The damage zone was limited to the first and second rows of grains. No damage was found beyond the third or fourth row of grains. Furthermore, grain sliding leading to grain-boundary fractures became more obvious in the severely deformed layer.

3.3.2.2. Fine-grained alumina. Figs 7c and 10a show the smooth groove formed by the blunt indenter. Similar to scratching coarse-grained alumina, the boundaries of the grains at the bottom of the groove were significantly weakened owing to the severe deformation, Fig. 10b. Grain sliding also took place. The width of the damage region was about 10 μm. The structure of the first row of grains was highly deformed, but the second and third rows possessed only a low density of dislocations (Fig. 10c). No dislocations were detected in and beyond the fourth row of grains. Hence, the depth of the zone affected by plastic deformation was about 3 μm. The density of dislocations was quite low here, because the blunt indenter reduced the level of the hydrostatic stress. As opposed to the sharp indenter no median or lateral cracks could be detected. Nor could the well-known cone cracks be observed.

3.4. Discussion and implication for ductile-regime grinding

In the following discussion, we make no distinction between the plastic and the damage zones and we use them interchangeably. Strictly speaking, a purely plastic zone should only contain a region of deformed grains inside which dislocations occur in certain slip systems and deformation twins develop. There should be no intergranular or transgranular cracks. However, due to the inhomogeneous dislocations and twins, microcracks may be found inside the grains and at grain boundaries. A damage zone encompasses both the inner plastic zone with associated microcracks and an outer zone of grain-boundary fractures where the grains may contain a low density of dislocations. It is therefore difficult to distinguish physically the purely plastic zone from the damage zone. In some cases the damage zone also includes median/lateral cracks (for a sharp indenter) and cone cracks (for a blunt indenter).

With the exception of the case of a sharp indenter on coarse-grained alumina, in all the other three cases investigated, the grains in the first row were always highly deformed during scratching, the material structure was changed, and the groove surfaces were smooth. All these observations strongly indicated that plastic deformation was a major mechanism of material removal.

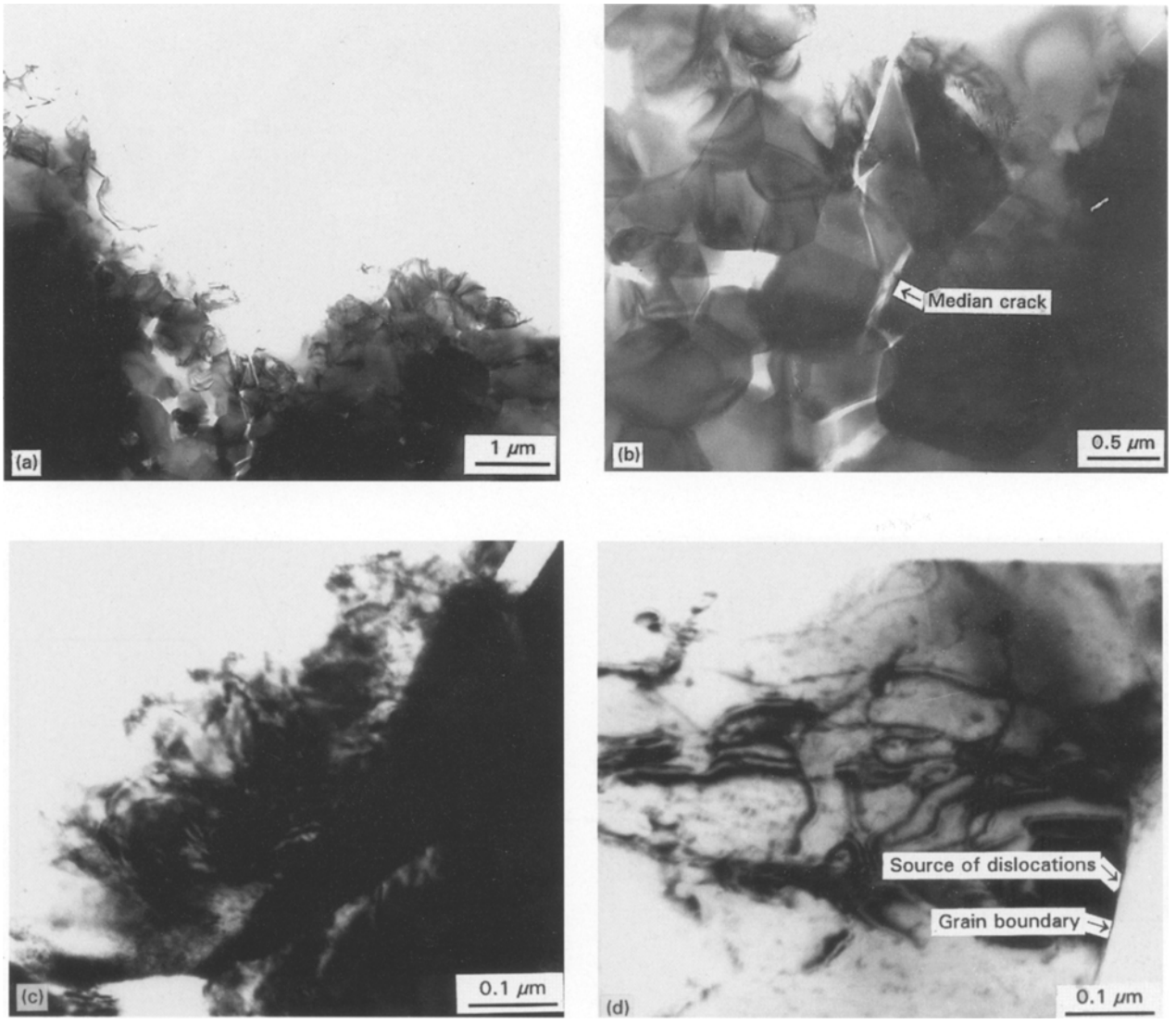

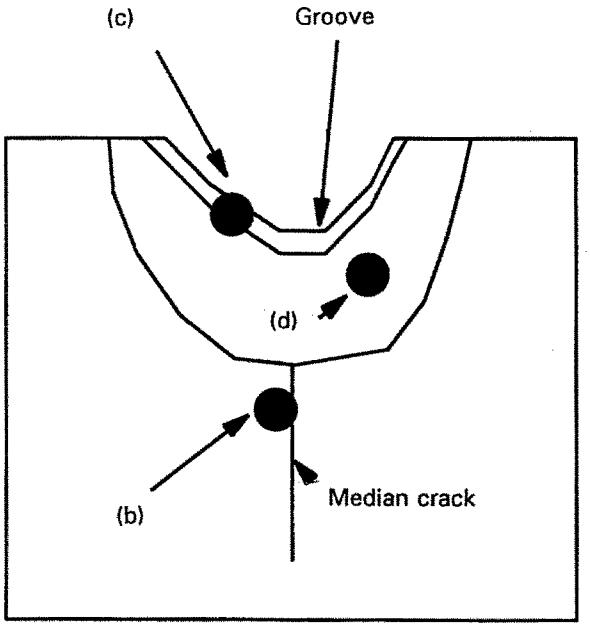

Figure 8 Scratching test with a Vickers indenter on fine-grained alumina. (a) Profile of the groove. The first row of grains is not seen in the picture. (b) Median crack beneath the plastic zone. Note that the median crack begins in the region with the deformed grains and extends past the undeformed grains. (c) The structure of the first deformed grains under the bottom of the groove. (d) Dislocation structure of the third to fifth rows of the grains.

Although the nature of the systems of dislocation in the severely deformed layer have not been explored, our experimental observations suggested that different slip systems were involved. However, the existence of slips could not guarantee the prevention of cracking. Most importantly, the subsurface damage must be considered even if the groove appears to be damage-free. The dimensions of the plastic or damage zone in the subsurface of a specimen depend on the type of indenter used (which alters the loading condition and thus the stress field in the material), and the grain size of the material (which determines the material's response to the applied stress).

The nature of the grain boundaries plays a significant role on the damage caused by scratching. A strong boundary between grains would offer a superior damage resistance. Because the fine-grained alumina had a higher boundary strength and was free of residual stresses relative to the coarse-grained alumina, for scratching with the sharp indenter, the depth of the damage zone was much smaller (i.e. 15 μm as opposed to 80 μm). The extent of grain

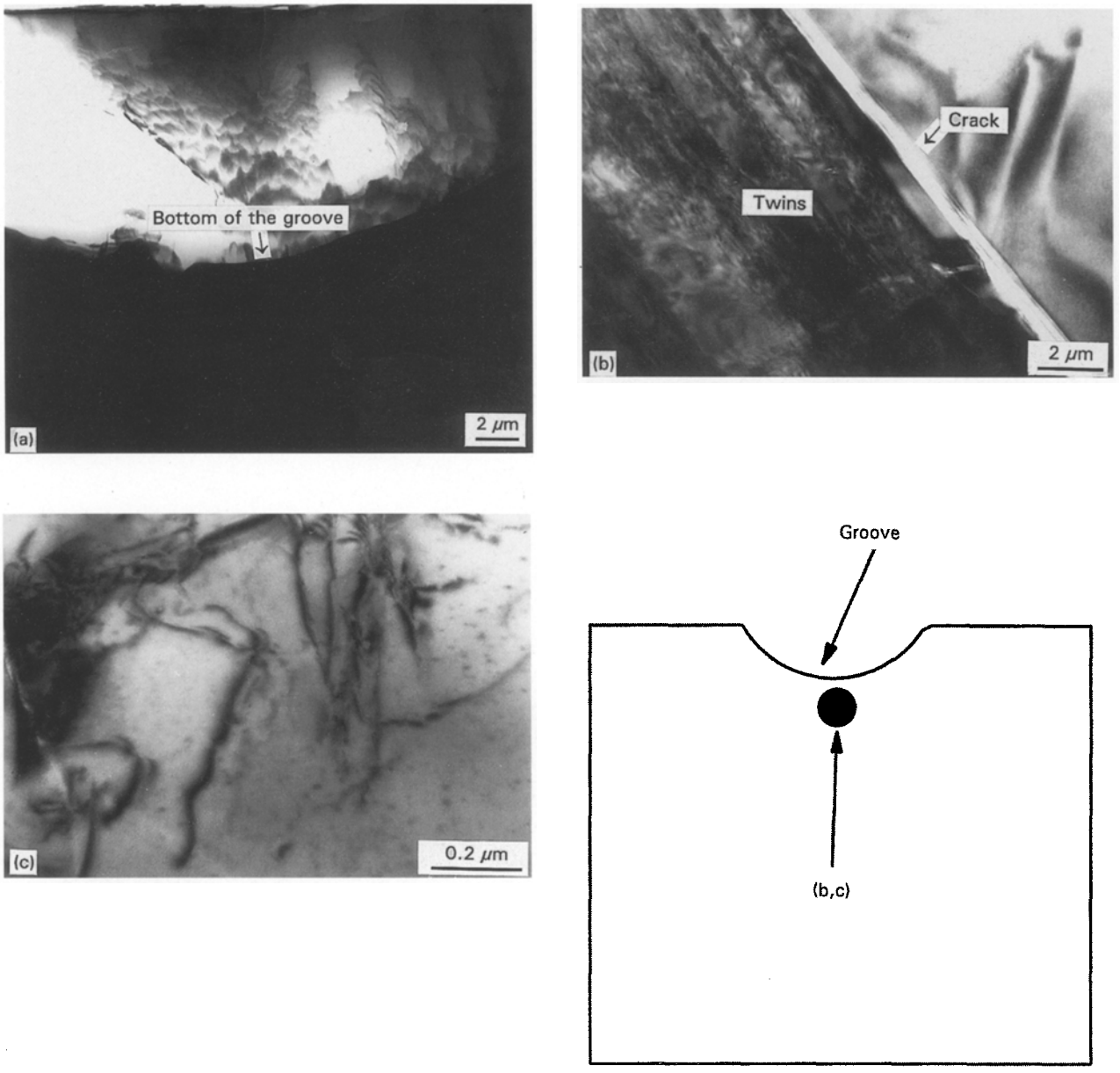

Figure 9 Scratching test with a blunt conical indenter on 25 μm coarse-grained alumina. (a) Profile of the groove; (b) rhombohedral twins in the plastic zone, note the crack along the twins; (c) dislocation structure of the plastic zone, individual dislocations can be distinguished.

sliding is also related to the strength of the grain boundaries. The aluminas studied in our experiments did not have a grain-boundary strength sufficient to prevent grain sliding leading to intergranular cracks in the severely deformed layer when a blunt indenter was used. Consequently, a purely plastic groove could not be achieved. It is noted that the grain boundaries have provided barriers for the spreading of the deformed structure. For example, the dislocations in the coarse-grained alumina were able to spread to a depth of 30 μm, while in the fine-grained ceramics it was only about 4 μm.

Now consider the different response of the two aluminas under the same scratching conditions. As discussed before, two special features were detected in the plastic or damage zone of the coarse-grained alumina: the appearance of rhombohedral twins and inhomogeneous distribution of dislocations. Because all the aluminas were prepared from the same powder and possessed the same crystallographic structure, the energy of activating twins must be the same. But the nucleation of twins in the coarse-grained alumina was easier because this material had a higher density of defects at the grain boundaries that acted as sites for initiation of twins. Consequently, the twins led to the inhomogeneous distribution of dislocations as the latter were concentrated at its boundaries [21]. An extremely high dislocation density in some places has led to crack formation as well as twins intersecting each other and at the grain boundaries. The formation of cracks underneath the groove in the coarse-grained alumina is strongly dependent on the structure of the plastic or damage zone. In the case of fine-grained alumina the absence of twins in the plastic zone and homogeneous dislocation distribution have prevented crack initiation inside the plastic zone. This fact leads to the conclusion that in evaluating the machinability of ceramic materials and the threshold of brittle–ductile transition, the subsurface structure of the plastic zone must be considered. Lawn *et al.* [22] recently

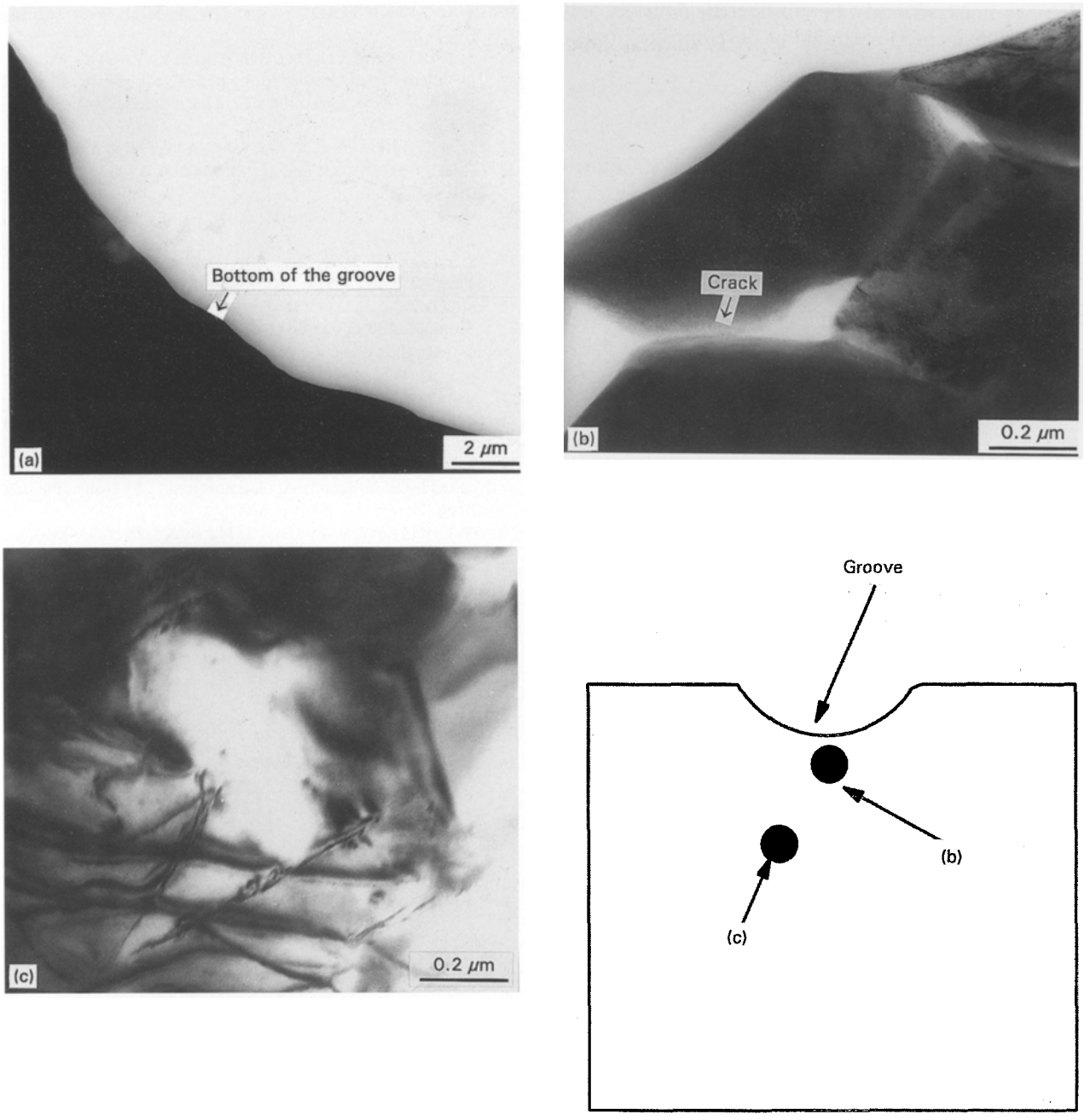

Figure 10 Scratching test with a conical blunt indenter on 1 μm fine-grained alumina. (a) Profile of the groove; (b) subsurface zone, note cracks under the first row of grains; (c) dislocation structure of the plastic zone.

discussed another type of brittle–ductile transition in which the microstructure is tailored to promote microfracture and other energy absorption mechanisms within a local zone under the indenter (instead of the usual cone fracture or median/lateral cracks) which gives a non-linear and hence psuedo "plastic" stress–strain curve. However, in ductile-regime grinding, such damage is not permitted and the "ductility" obtained is not relevant for damage-free machining.

4. Conclusions

1. Plastic zones were discovered during scratching alumina under different sliding conditions. The dimensions and structure of such plastic zones depended greatly on the types of alumina and indenters used.

2. The plastic zone in the coarse-grained alumina (25 μm) was characterized by twins and a high density of dislocations produced by different slip systems. However, in the fine-grained alumina (1 μm) there was a much lower density of dislocations.

3. The existence of rhombohedral twins and inhomogeneous distribution of dislocations in the coarse-grained alumina were the sources of cracking inside the plastic zone.

4. The initial microstructure of the alumina influenced to a great extent its response to scratching. The stacking faults on the grain boundaries of the coarse-grained alumina due to sintering led to easy separation of grains and the formation of a large damage zone.

5. Surface examination by SEM could not guarantee real damage-free scratching or grinding. The subsurface

damage must seriously be considered. A better and more reliable criterion should be developed to predict real damage-free grinding.

Acknowledgements

The authors thank the Australian Research Council (ARC) for continuing support of this project. I. Z. is supported by an ARC Postgraduate Research Award. The University of Sydney Electron Microscopy Unit is thanked for the use of its facilities.

References

1. L. ZHANG, in "International Ceramics Monographs", edited by C. C. Sorrell and A. J. Ruys (Australian Ceramic Society, Sydney, 1994) p. 1377.
2. E. BRINKSMEIER and P. ROTH, in "Proceedings of 7th Annual Meeting ASPE" (American Society for Precision Engineering, Florida, 1992) p. 73.
3. M. SMITH and O. SCATTERGOOD, *ibid.*, p. 37.
4. G. BIFANO, K. DEPIERO and D. GOLINI, *Precision Eng.* **15** (1993) 238.
5. L. ZHANG, *Int. J. Mach. Tool Manufact.* **34** (1994) 1045.
6. L. ZHANG, T. SUTO, H. NOGUCHI and T. WAIDA, *Manuf. Rev.* **5** (1992) 261.
7. *Idem, Int. J. Machin. Tools Manufact.* **33** (1993) 230.
8. L. ZHANG and Y.-W. MAI, in "Proceedings of the 8th Annual Meeting ASPE" (Seattle, 1993) p. 230.
9. A. K. MUKHOPADHYAY, Y.-W. MAI and S. LATHABAI, in "Ceramics", Vol. 2. edited by M. J. Bannister (CSIRO, Melbourne, 1992) p. 910.
10. A. K. MUKHOPADHYAY and Y.-W. MAI, *Wear* **162–164** (1993) 258.
11. A. J. BUSHBY, A. K. MUKHOPADHYAY and Y.-W. MAI, in "International Ceramic Monographs", edited by C. C. Sorrel and A. J. Ruys (Australian Ceramic Society, Sydney, 1994) p. 638.
12. M. V. SWAIN, *Proc. R. Soc. Lond.* **A366** (1979) 575.
13. H. K. TÖNSHOFF and H. TRUMPOLD, *Ann. CIRP* **378** (1989) 699.
14. W. S. BLACKLEY and R. O. SCATTERGOOD, *Precision Eng.* **13** (1991) 95.
15. S. S. CHANG, D. B. MARSHAL and A. G. EVANS, *J. Appl. Phys.* **32** (1982) 298.
16. L. ZHANG and M. MAHDI, in "International Ceramics Monographs", edited by C. C. Sorrel and A. J. Ruys (Australian Ceramic Society, Sydney, 1994) p. 644.
17. B. R. LAWN, "Fracture of brittle solids" (Cambridge University Press, Cambridge, 1993).
18. B. J. HOCKEY and B. R. LAWN, *J. Mater. Sci.* **10** (1975) 1275.
19. B. J. HOCKEY, in "Fracture Mechanics of Ceramics", Vol. 6, edited by R. C. Brandt, A. G. Evans and F. F. Lange (Plenum Press, New York, 1982) p. 637.
20. D. E. KIM and N. P. SUH, *J. Mater. Sci.* **28** (1993) 3895.
21. K. PETER, D. LAGERLOF and A. H. HEUER, *J. Am. Ceram. Soc.* **28** (1993) 3895.
22. B. R. LAWN, N. P. PADTURE, H. CAI and F. GUIBERTEAU, *Science* **263** (1994) 118.

Received 22 December 1994
and accepted 15 March 1995